Spectroscopic Evidence for the Formation of Four-Stranded Solution Structure of Oligodeoxycytidine Phosphorothioate†

Hideyuki Kanehara, Masatsugu Mizuguchi, Kunihiko Tajima, Kenji Kanaori, and Keisuke Makino*

Department of Polymer Science and Engineering, Kyoto Institute of Technology, Matsugasaki, Sakyo-ku, Kyoto 606, Japan

Received June 24, 1996; Revised Manuscript Received December 6, 1996⊗

ABSTRACT: Oligodeoxycytidine phosphorothioate (PS-dC$_n$, n = chain length), known to show virus inhibition ability by a mechanism other than the antisense one when $n \approx 20$, was explored for its solution structure by circular dichroism (CD) and ultraviolet (UV) absorption spectroscopy. For PS-dC$_4$, when the strand concentration was higher than 10 μM, the respective 288-nm positive and 265-nm negative peaks appeared in the CD spectra at slightly acidic pHs and 0 °C in the absence of salt, which is indicative of a four-stranded structure (namely, the i-motif). Strand concentration-dependent CD spectroscopy indicated that intermolecular association is responsible for this i-motif. The formation of i-motif was also characterized by UV absorption spectroscopy, in which the dissociation of this structure caused a sharp increase in the absorbance at 275 nm and a decrease at 305 nm. By plotting this change, the T_m values were estimated to be ca. 11 and 13 °C at 20 and 50 μM strand concentrations, respectively. Stability of the i-motif was compared between PS-dC$_4$ P-chiral diastereoisomers, and the S_p configuration produced a more stable structure than R_p. PS-dC$_{20}$ was also investigated at physiological temperature, and the respective 288-nm positive and 265-nm negative peaks appeared at slightly acidic pH; it has been suggested that intermolecular folding was predominant above ca. 1 μM and that intramolecular folding dominated at low strand concentrations such as 0.05 μM. Gel-filtration chromatography and nondenaturing gel electrophoresis provided the supporting data for the four-stranded folding of PS-dC$_{20}$.

Oligodeoxynucleoside phosphorothioate (PS-oligo),[1] in which one of the nonbridging oxygen atoms in each internucleotide phosphate linkage is replaced by a sulfur atom, has been used extensively as an antisense molecule, and it has been demonstrated in a number of papers that this molecule is potentially antiretroviral (Agrawal et al., 1988; Majumdar et al., 1989; Stein & Cheng, 1993). In the antisense method, an antisense PS-oligo commonly has a base sequence complementary to that of its target mRNA and inhibits gene expression by forming a hybrid with the mRNA. However, an exceptional case was also reported where oligodeoxycytidine phosphorothioate (PS-dC$_n$, n = chain length), which has no complementary sequence against the target, showed efficient HIV inhibition (Matsukura et al., 1987, 1988). This result strongly indicates the coexistence of some unidentified mechanisms other than the antisense one, possibly characteristic of PS-dC$_n$. To reveal the entire antiviral mechanism of PS-oligo, it is worthwhile exploring such unique properties of PS-dC$_n$.

It has been known that natural-type poly(dC) (PO-dC$_n$) forms a duplex by three hydrogen bonds between protonated and nonprotonated cytosine moieties at slightly acidic pH (Guschlbauer, 1967; Hartman & Rich, 1965; Slegers & Fiers, 1973). Recently, it was demonstrated by ultraviolet (UV) melting profile and nondenaturing gel electrophoretic migration that C-rich oligodeoxynucleotides (PO-oligos) such as d(CCCCAA)$_4$, d(CCCCAAAA)$_4$, etc., form a structure other than a duplex under acidic conditions (Ahmed & Henderson, 1992). NMR analysis carried out for d(TCCCCC) at pH 4.3 presented unusual interresidue sugar−sugar NOE cross peaks for H1′-H1′, H1′-H2″, and H1′-H4′, which are not detected for a conventional DNA duplex (Gehring et al., 1993; Leroy et al., 1993). This unique structure of such C-rich PO-oligos has been identified as a four-stranded complex, namely, an i-motif. In this structure, two base-paired parallel-stranded duplexes are associated, their base pairs fully intercalated, and the relative orientation of the duplexes is antiparallel. Furthermore, it was reported (Leroy et al., 1994) that longer C-rich PO-oligos such as d[(CCCTAA)$_3$CCC], part of a vertebrate telomeric DNA sequence, formed i-motif structures at neutral or weakly acidic pH, and the authors suggested that this structure is possible even *in vivo*. Such a unique i-motif structure was also observed for C-rich PO-oligo derived from many cellular genes, such as a telomeric repeating sequence of d[(CCCTAA)$_3$CCCT] existing in the chromosomes of humans and vertebrates, a rat c-Ki-*ras* protooncogene promoter sequence of d[GC(TCCC)$_3$TCCT(TCCC)$_3$], and so on, by measuring pH and temperature profiles with circular dichroism (CD) and polyacrylamide gel electrophoretic mobility, and so on (Manzini et al., 1994). Recently the i-motif was finally confirmed by X-ray analysis (Chen et al., 1994).

In the present study, with the aim of examining if PS-dC$_n$ also forms such a unique structure, we employed CD (Manzini et al., 1994) and UV (Mergny et al., 1995) spectroscopy, both of which recognize protonated and

† This work was supported partly by a Grant-in-Aid for Scientific Research (08458176) from the Ministry of Education, Science and Culture and by Rational Drug Design Laboratories.

* To whom correspondence should be addressed.

⊗ Abstract published in *Advance ACS Abstracts,* February 1, 1997.

[1] Abbreviations: PS-oligo, oligodeoxynucleoside phosphorothioate; PO-oligo, natural-type oligodeoxynucleotide; PS-dC$_n$, oligodeoxycytidine phosphorothioate; PO-dC$_n$, natural-type oligodeoxycytidine; CD, circular dichroism; RPLC, reversed-phase liquid chromatography; IELC, ion-exchange liquid chromatography; PNK, T4 polynucleotide kinase; EDTA, ethylenediaminetetraacetic acid.

S0006-2960(96)01528-0 CCC: $14.00

nonprotonated cytidine base pairing in the four-stranded structure: It should be noted that NMR, one of the most powerful spectroscopic techniques, could not be readily applied to PS-dC$_n$ due to the complex overlap of the proton signals of the P-chiral diastereoisomers. Also, we obtained supporting data by gel-filtration chromatography and nondenaturing gel electrophoresis.

In PS-oligo, P-chirality of an internucleotide phosphorothioate linkage (R_p and S_p) generates diastereoisomers the number of which increases in proportion to 2^{n-1} (n = number of phosphorothioates) (Stec et al., 1984). This difference in the configuration produces different types of PS-oligo diastereoisomers (Stec & Wilk, 1994). According to previous papers (Kanehara et al., 1996a; Koziolkiewicz, et al., 1995; LaPlanche et al., 1986; Stec et al., 1995; Stein et al., 1988), for instance, the S_p isomer exhibited higher duplex stability than R_p when DNA was used as a target, while such a clear trend was not seen when RNA was a target. Another interest in the present study is, therefore, to see if the i-motif PS-dC$_n$ structure is dependent on the P-chiral diastereoisomers.

MATERIALS AND METHODS

Sample Preparation. Both PO- and PS-oligo were synthesized on Milligen/Biosearch Cyclone Plus DNA synthesizer by the standard phosphoramidite methods employing β-cyanoethyl phosphoramidite monomers. All reagents and solvents used for the synthesis were purchased from the same company. Synthesis was carried out on the 1-μmol scale. Oligodeoxynucleoside phosphoramidites were treated either with iodine or with tetraethylthiuram disulfide to generate phosphodiester and phosphorothioate linkages, respectively. Deprotection of the oligomers was performed in concentrated NH_3 for 7 h at 55 °C. After NH_3 evaporation, the oligomers were purified by reversed-phase liquid (RPLC) and DEAE ion-exchange (IELC) chromatography (Agrawal et al., 1990; Kanehara et al., 1996b; Stec et al., 1985; Zon, 1987) using an HPLC system consisting of an SCL-6B system controller, an SPD-M 6A photodiode array UV−vis detector, a pair of LC-6A pumps, and a PC-9801 RA51 host computer (Shimadzu, Japan). The RPLC columns used were RP-8(e) (4 μm, 4.6 × 250 mm) (Merck, Germany) and Wakosil 5C18 (5 μm, 4.6 × 150 mm) (Wako, Japan). Other RPLC conditions are as follows: eluents, (A) 0.1 M triethylammonium acetate (pH 7.0) and (B) 0.1 M triethylammonium acetate (pH 7.0)/acetonitrile (50/50 v/v); gradient, 10−40% B (linear) for 25 min and then 50% B and 40−100% B (linear) for 10 min for DMTr on and -off samples, respectively; flow rate, 0.7 mL/min; detection, 254 nm; temperature, ambient. For IELC, the HPLC system used was same as that used for RPLC and the column used was TSK-GEL DEAE-2SW (10 μm, 4.6 × 250 mm) (Tosoh, Japan). Other chromatographic conditions are as follows: eluent, (A) 50 mM ammonium acetate and (B) 1.5 M ammonium acetate; gradient, 0−100% B (linear) for 60 min; flow rate, 1 mL/min; detection, 254 nm; temperature, ambient. Unless otherwise specified, PS-dC$_4$ was used as a diastereomeric mixture.

For the separation of PS-dC$_4$ diastereoisomers arising from the three P-chiral internucleotide phosphorothioate linkages, a combination of RPLC and IELC was used. A diastereomeric mixture of detritylated PS-dC$_4$ was first isolated in a single peak by IELC, and subsequently eight diastereoisomers included in the IELC envelope peak separated in seven peaks by RPLC. The specific configuration of each diastereoisomer in the RPLC peaks was already identified previously (Wilk & Stec, 1995), and therefore, we assigned each peak accordingly: The elution order was $R_pR_pR_p$ > $R_pR_pS_p$ = $S_pR_pR_p$ > $S_pR_pS_p$ > $R_pS_pR_p$ > $S_pS_pR_p$ > $R_pS_pS_p$ > $S_pS_pS_p$. This elution order is consistent with that reported previously for diastereoisomers of a PS-oligo tetramer [d($A_{ps}T_{ps}C_{ps}G$), ps = phosphorothioate], which were separated by similar RPLC (Murakami et al., 1994). For further confirmation of the three diastereoisomers ($R_pR_pR_p$, $S_pR_pS_p$, and $S_pS_pS_p$) which were used for the following spectroscopical measurements, stereodifferential enzymatic digestions (Burgers & Eckstein, 1978) were carried out, in which only the R_p phosphorothioates are specifically digested by snake venom phosphodiesterase (Pharmacia, Sweden) and the remaining free phosphorothioate at the 5′-end is removed by calf intestine alkaline phosphatase (Toyobo, Japan). Each isolated diastereoisomer was dissolved in a mixture of 100 mM Tris-HCl buffer (50 μL, pH 8.9), 20 mM $MgCl_2$ (5 μL), and the enzymes (20 μL of 250 units/mL snake venom phosphodiesterase and 6 μL of 2 units/mL alkaline phosphatase). The reaction mixtures were incubated for 1 h at 37 °C and analyzed by RPLC employing the same conditions as used for the isomer separation. For $R_pR_pR_p$ and $S_pS_pS_p$ diastereoisomers, only the cytidine and the parent RPLC peaks were observed, respectively. For the $S_pR_pS_p$ diastereoisomer, the parent peak was eliminated and simultaneously the faster-eluting peak appeared, which was attributed to [S_p]-dC_{ps}C by comparison with a genuine sample (Koziolkiewicz et al., 1986). These results confirm our assignment.

The concentrations of PO- and PS-dC$_n$ sample solutions used in the following measurements were estimated using the extinction coefficients at 260 nm which were calculated by the nearest-neighbor method (Fasman, 1975). The pH adjustment of the sample solutions was performed with 0.01 and 0.1 N NaOH and HCl.

UV and CD Spectroscopy. UV absorption spectra (200−350 nm) were recorded with a UV-260 spectrophotometer (Shimadzu). The optical path length of the cell was 1 cm. The sample temperature was controlled by the thermoblock buried in the sample holder which was coupled with the thermocouple. After each change of the temperature settings, samples were allowed to stand for 20 min for the next measurements. CD spectra were measured over 210−320 nm on a J-720 spectropolarimeter (Japan Spectroscopic Co., Japan) using jacketed quartz cells with the optical path lengths of 1 and 10 cm. The CD cell temperature was regulated by circulating an ethylene glycol/water mixture in the jacket, whose temperature was controlled by an RTE-100 thermostat (NESLAB, Japan). After each temperature change, samples were allowed to stand for 20 min for the next measurements. For both spectroscopy, samples were premelted at 75−80 °C immediately prior to the measurements to destroy secondary structure and then allowed to thermally equilibrate.

Gel-Filtration Chromatography. Gel-filtration chromatography was performed using a CCPM-II pumping system coupled with an SC-8020 system controller and a UV-8020 detector (Tosoh). The column used was TSK-G3000PW (10 μm, 8 × 600 mm). Other chromatographic conditions are

as follows: sample size, 5 μL (1 mM); eluent, 20 mM acetate buffer (pH 4.5) containing 0.3 M NaCl; flow rate, 0.8 mL/min; detection, 305 nm; temperature, ambient.

Nondenaturing Polyacrylamide Gel Electrophoresis. Sample oligodeoxynucleotides, PS-dC_{20} and PO-dT_{20}, were radiolabeled with T4 polynucleotide kinase (PNK) (10 000 units/mL, New England Biolabs) and ^{32}P-ATP (5000 Ci/mmol, Amersham, England). Other reagents used were of gel electrophoresis grade. The reaction mixtures consisting of 1 μL of PNK, 6 μL of [^{32}P]ATP, 1 μL of protruding buffer (New England Biolabs), and 2 μL of a stock sample solution (strand concentration being 5 μM) were incubated at 37 °C for 30 min. After incubation, ethylenediaminetetraacetic acid (EDTA) was added to terminate the reaction, and subsequently unreacted [^{32}P]ATP, enzyme, and salt were removed with Sep-Pak Cartridges (Waters). After drying with a centrifugal concentrator (Tomy, Japan), loading samples were prepared. The final composition was as follows: ^{32}P-labeled PS-dC_{20} and PO-dT_{20} (8 nM) + nonlabeled PS-dC_{20} and PO-dT_{20} (10 μM), respectively; buffer, 50 mM Tris-acetate (pH 4.5) containing 0.5 mM EDTA and 5% glycerol. Aliquots (4 μL) were loaded on the nondenaturing 20% polyacrylamide gel. Electrophoretic measurements were carried out in the same buffer as for the samples for 6 h at 10 °C under recirculation of the buffer. After the gelwas dried, an autoradiogram was obtained.

RESULTS

A specific Cotton effect appearing in the CD spectra of C-rich PO-oligo is informative of protonated and nonprotonated cytosine base-pairing (Edwards et al., 1988, 1990), and an enlarged positive peak with a red shift and a concomitant negative peak are indicative of the i-motif structure of C-rich PO-oligo (Manzini et al., 1994). When this structure collapses, this positive peak is lowered with a blue shift and simultaneously the negative peak disappears. Similarly UV spectra show a characteristic temperature-dependent blue shift, indicative of the thermal dissociation of the i-motif structure (Mergny et al., 1995). In the present study, therefore, we applied these spectroscopic techniques to PS-dC_n.

CD Spectra of PS-dC_4 as a Function of pH. i-Motif structure formation has been reported to depend on the surrounding conditions, particularly on the pH (Manzini et al., 1994; Mergny et al., 1995). First, therefore, pH-dependent CD spectroscopy was carried out for PS-dC_4 (25 μM) at 0 °C. The reason that we took this small PS-oligo is to simplify the system by avoiding the contribution of intramolecular folding. Salt destabilizes the i-motif (Mergny et al., 1995), and to increase the association of this small oligonucleotide, therefore, measurements were performed in the absence of salt. As shown in Figure 1a, this sample showed both the 288-nm positive and 265-nm negative peaks at pH 4.5, while at higher (pH 7.0) and lower (pH 3.0) pHs, the positive peak decreased with blue shifts to 278 and 285 nm, respectively, and the concomitant negative peak disappeared.

UV and CD Spectra of PS-dC_4 as a Function of Temperature and Strand Concentration. Influences of other conditions on the association of PS-dC_4 were also explored. Temperature elevation causes unfolding of the i-motif structure of C-rich PO-oligo as is seen for conventional DNA

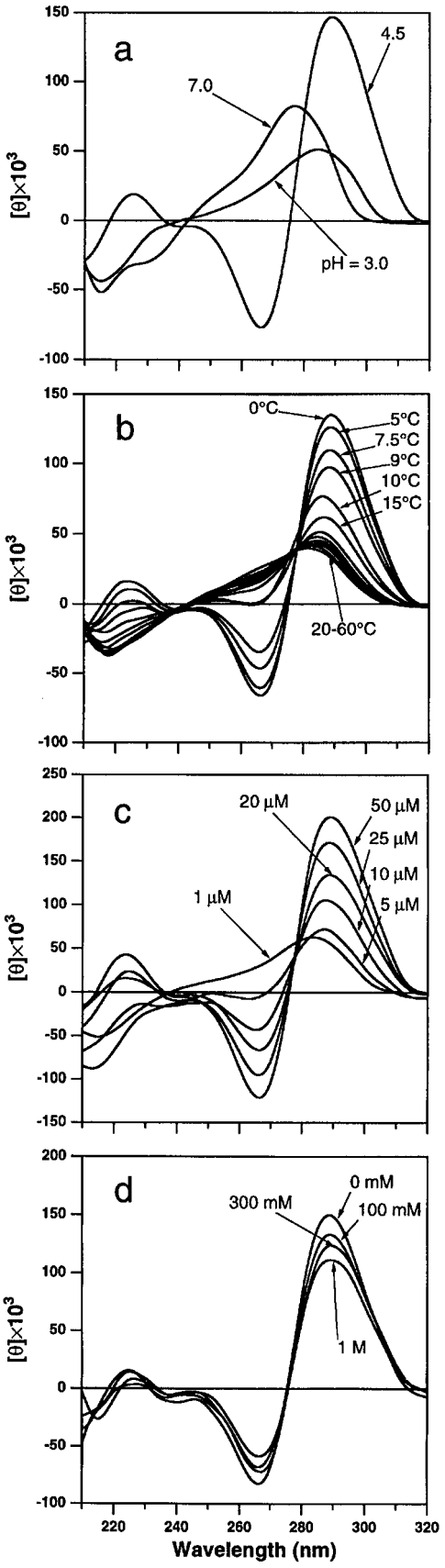

FIGURE 1: CD spectra obtained for PS-dC_4. (a) Effect of pH. Conditions: strand concentration, 25 μM; temperature, 0 °C; pH, 3.0, 4.5, and 7.0. (b) Effect of temperature. Conditions: strand concentration, 20 μM; temperature, 0−60 °C; pH, 4.5. (c) Effect of strand concentration. Conditions: strand concentration; 1−20 μM; temperature, 0 °C; pH, 4.5. (d) Effect of NaCl concentration. Conditions: strand concentration, 20 μM; temperature, 0 °C; pH, 4.5; salt concentration, 0−1 M.

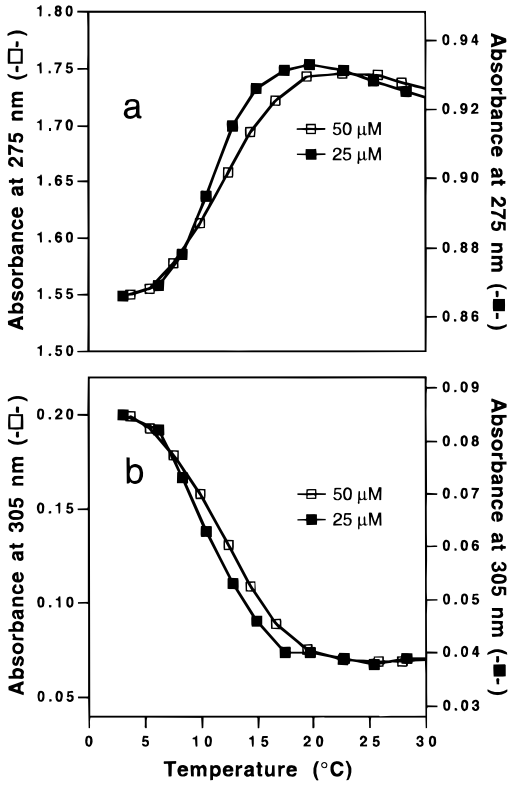

FIGURE 2: UV denaturation profiles obtained for PS-dC$_4$ at (a) 275 nm and (b) 305 nm. Conditions: strand concentration, 20 (closed squares) and 50 μM (open squares); pH, 4.5. From the spectral change, the T_m values were obtained to be ca. 11 and 13 °C at the strand concentrations of 20 and 50 μM and the isosbestic point of this equilibrium to be at ca. 290 nm.

double strands. Temperature-dependent CD and UV spectroscopy was, therefore, performed for PS-dC$_4$ at pH 4.5. The strand concentrations were 20 and 25 μM for CD and UV spectroscopy, respectively. The CD spectral change obtained at 0−60 °C is represented in Figure 1b. Both the positive and negative peaks appeared below 10 °C and became smaller as the temperature was elevated. UV measurements were also conducted in the 0−60 °C temperature range, and the respective increase and decrease of the absorbance at 275 and 305 nm was observed as a function of temperature. The isosbestic point was obtained at 292 nm (data not shown). By plotting the absorbance at the both wavelengths against temperature, the thermal dissociation UV profile was obtained, as shown in Figure 2 (closed squares). Using this plot, the T_m value was determined to be ca. 11 °C. To see if the thermal stability is concentration-dependent, which allows us to determine whether this folding is due to intra- or intermolecular interaction, analogous UV measurements were carried out at the increased strand concentration of 50 μM. The resultant dissociation profile is also depicted in Figure 2b (open squares). The curve is shifted toward the higher T_m compared to that obtained at 25 μM. The T_m value estimated from this curve is ca. 13 °C. To see the strand concentration effect on the structure of PS-dC$_4$ in more detail, we also explored the CD spectral change at pH 4.5 and at 0 °C. The strand concentration was varied from 1 to 50 μM. The resulting spectra are shown in Figure 1c. Above 10 μM, both the positive and negative peaks clearly appeared at 288 and 265 nm, respectively, while below 1 μM, the negative peaks completely disappeared and only the 280-nm positive peak remained.

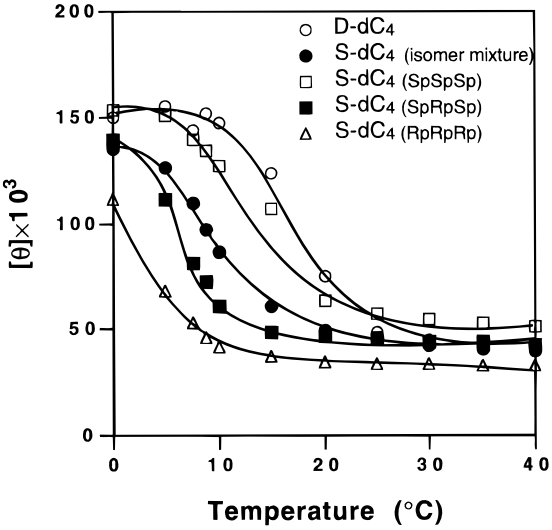

FIGURE 3: Change in the molar ellipticity at 288 nm as a function of temperature for PO-dC$_4$ (open circles), a diastereomeric mixture of PS-dC$_4$ (closed circles), and PS-dC$_4$ with a configuration of $S_pS_pS_p$ (open squares), $S_pR_pS_p$ (closed squares), and $R_pR_pR_p$ (open triangles). Conditions: strand concentration, 20 μM; temperature, 0 °C; pH, 4.5.

Effect of Salt on CD Spectra of PS-dC$_4$. It has been demonstrated that salt destabilizes the i-motif structure of C-rich PO-oligos (Mergny et al., 1995). To see if this occurs for the PS-oligo i-motif, therefore, CD measurements were conducted for PS-dC$_4$ (20 μM) in the presence of NaCl at pH 4.5 and 0 °C. The NaCl concentration ranged up to 1 M. As the salt concentration was increased, both the positive and negative peaks decreased gradually, as depicted in Figure 1d.

CD Spectra of PS-dC$_4$ Diastereoisomers. To compare the thermal stability of the i-motif structure between the P-chiral diastereoisomers, CD spectroscopy was carried out at varied temperatures at pH 4.5 for the isolated PS-dC$_4$ diastereoisomers whose configurations are $S_pS_pS_p$, $S_pR_pS_p$, and $R_pR_pR_p$. The strand concentration was 20 μM. As reference molecules, we took PO-dC$_4$ and a diastereomeric mixture of PS-dC$_4$. The CD melting profiles were obtained by plotting the molar ellipticity at 288 nm against temperature, as represented in Figure 3. Although overall thermal dissociation curves could not be obtained for these samples because of the low T_m values, this measurement demonstrated a clear difference in the thermal stability of these samples. The order of the T_m values was PO-dC$_4$ > $S_pS_pS_p$ > PS-dC$_4$ diastereoisomer mixture > $S_pR_pS_p$ > $R_pR_pR_p$.

CD Spectroscopy, Gel-Filtration Chromatography, and Nondenaturing Gel Electrophoresis of PS-dC$_{20}$. In the case of DNA/DNA and PS-oligo/DNA duplexes, stability increases with increase in the chain length of the strands. To see the influence of the chain length on the i-motif structure of PS-oligo, we employed a larger sample of PS-dC$_{20}$. First, we carried out CD spectroscopy at 0 °C under conditions similar to those used for PS-dC$_4$, and great improvement of the thermal stability was observed (data not shown). Also, at 25 °C, this molecule (6 μM) showed both positive and concomitant negative peaks in the pH 5.6−6.9 range in the absence of salt (data not shown). So we were interested in the folding behavior of this molecule under physiological conditions and performed CD measurements at 37 °C in the presence of 0.9 wt % NaCl. As shown in Figure 4a, PS-

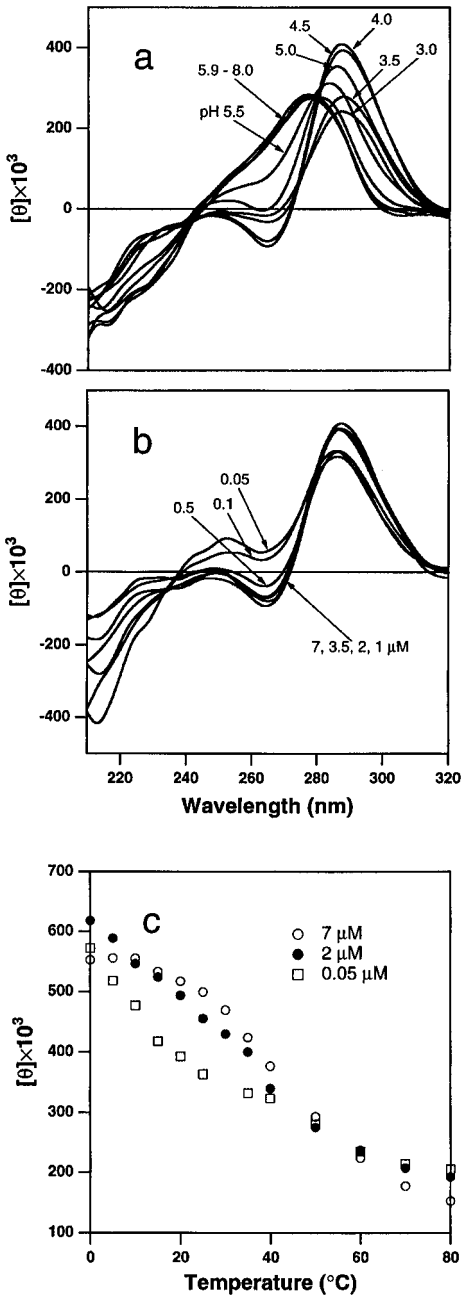

FIGURE 4: CD spectra obtained for a diastereomeric mixture of PS-dC_{20} at 37 °C as a function of (a) pH (strand concentration 2 μM) and (b) strand concentration (pH 4.5). (c) Thermal dissociation profiles obtained at 0.05 and 2 μM strand concentrations at pH 4.5.

dC_{20} (2 μM) exhibited both the 288-nm positive and 265-nm negative peaks below pH 5.0, although below pH 3.0, the intensities of both the positive and negative peaks decreased simultaneously. Also, at pH 4.5 and in the presence of NaCl, concentration-dependent CD spectroscopy was carried out by varying the strand concentration from 0.05 to 7 μM. The resultant CD spectra are shown in Figure 4b. Under these conditions, the 288-nm positive and concomitant 265-nm negative peaks appeared above 0.5 μM. Compared to the results for PS-dC_4, unexpectedly, all of the CD spectra were identical in this concentration range. We obtained thermal dissociation profiles to see if such behavior occurs only at this temperature incidentally. The resultant CD thermal dissociation profiles are represented in Figure 4c. As is seen in the figure, at strand concentrations of 2 and 7 μM, T_m profiles were dependent on the strand concentration, thus implying that the coincidence mentioned above was incidental. On the other hand, at 0.1 and 0.05 μM, the 285-nm positive peak was slightly lowered and simultaneously the much smaller negative peak was obtained, although the molar ellipticity was not on the minus side. Also it was found that the intensity of the positive peak generated at 0.05 μM was temperature-dependent as shown in Figure 4c.

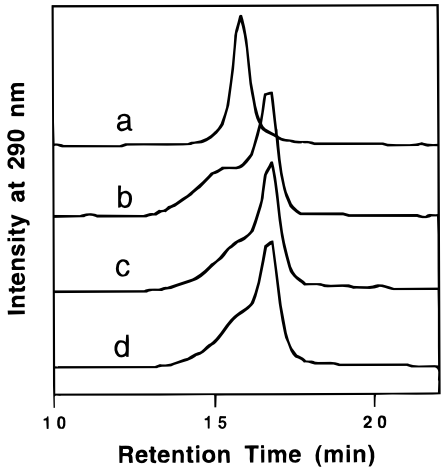

FIGURE 5: Gel-filtration chromatography obtained for (a) PO-dT_{20}, (b) PO-dC_{20}, and (c) PS-dC_{20}, which were annealed by heating the sample at 100 °C and cooled slowly for 1 h to the room temperature. Nonannealed PS-dC_{20} (d) was prepared by heating at 100 °C and cooled down to 0 °C instantly. Chromatographic conditions: sample size, 5 μL (1 mM); column, G3000PW (10 μm, 8 × 600 mm); eluent, 20 mM acetate buffer (pH 4.5) containing 0.3 M NaCl; flow rate, 0.8 mL/min; detection, 305 nm; temperature, ambient.

Molecular size distribution of PS-dC_{20} four-stranded complexes was measured by gel-filtration chromatography. As references, PO-dT_{20} and PO-dC_{20} were also chromatographed. Immediately prior to the measurements, PS-dC_{20}, PO-dT_{20}, and PO-dC_{20} were annealed by heating at 100 °C and cooling down slowly for 1 h to the room temperature. As depicted in Figure 5, as expected, PO-dT_{20} produced a single peak; however, PO-dC_{20} gave two peaks, the first peak of which was broadened. In the case of PS-dC_{20}, the peak shape was analogous to that of PO-dC_{20}. Also, PS-dC_{20} that was heated at 100 °C and instantly cooled down to 0 °C was loaded and a similar peak shape was obtained. Nondenaturing gel electrophoresis, which also analyzes the size of the folded oligonucleotides, was conducted for annealed and nonannealed PS-dC_{20} as well as for PO-dT_{20} as a reference. Although a strong band was not obtained readily for PS-dC_{20} but only for PO-dT_{20} in the autoradiograms, since PS-dC_{20} is not a good substrate for PNK, a slowly migrating band, compared to the clear band of PO-dT_{20}, emerged for both annealed and nonannealed PS-dC_{20} (data not shown).

DISCUSSION

Formation of i-Motif PS-dC_4 Structure and Its Thermal Dissociation. It has been demonstrated previously that formation of i-motif PO-dC_n structure depends on pH and that this structure is stable at slightly acidic pHs (Gehring et al., 1993; Leroy et al., 1994; Manzini et al., 1994; Mergny et al., 1995), and that appearance of both positive and negative peaks in the CD spectrum is indicative of the i-motif PO-dC_n formation (Manzini et al., 1994). We began pH-

dependent CD spectroscopy with a short strand such as PS-dC$_2$ (25 μM) at 0 °C in the absence of salt. Compared to the result obtained at pH 7.0, we observed neither an increase in the intensity of the positive peak nor generation of a negative peak at slightly acidic pHs, although the positive peak was shifted from 275 to 285 nm (data not shown), thus suggesting that PS-dC$_2$ is not sufficiently large to form the i-motif structure under the present conditions. On the other hand, PS-dC$_4$ (25 μM) showed both the increased 288-nm positive and concomitant 265-nm negative peaks at pH 4.5, which are characteristic of i-motif structure (Figure 1a). The shift of the positive peak and the disappearance of the negative peak at higher (pH 7.0) and lower (pH 3.0) pH implies that the i-motif structure was destroyed in such pH regions. These observations agree with the results reported previously for the i-motif formation of C-rich PO-oligos (Gehring et al., 1993; Manzini et al., 1994). In order to see if this behavior is characteristic of PS-dC$_4$, we employed oligodeoxythymidine phosphorothioate (PS-dT$_4$) as a reference and carried out analogous CD measurements over similar pH range. PS-dT$_4$ did not show such a spectral pattern at any pH but weak positive peaks around 275 nm.

It has been reported for C-rich PO-oligos that strand concentrations are highly responsible for the i-motif formation. In the case of d(TCCCCC), for instance, it was demonstrated using electrophoretic analysis that the i-motif was stable at 2 °C when the strand concentrations was roughly above 30 μM (Gehring et al., 1993; Leroy et al., 1993). In our present CD spectroscopical measurements, a Cotton effect indicative of i-motif formation appeared for PS-dC$_4$ over the 10−50 μM strand concentration range at pH 4.5 and 0 °C (Figure 1c). This observation is consistent with the previous result mentioned above. The data shown in Figure 4c also show that the i-motif structure of PS-dC$_4$ collapses below 1 μM. Consequently complete i-motif formation of PS-dC$_4$ requires at least ca. 10 μM strand concentration. Thus, similarly to the previous results for C-rich PO-oligos, it is evident that PS-dC$_4$ can form the i-motif.

The thermal dissociation CD profile obtained for PS-dC$_4$ (Figure 1b) indicates that this i-motif structure is stable below 10 °C at the strand concentration of 25 μM and destroyed above this temperature. This observation is consistent with the result reported for C-rich PO-oligos previously (Leroy et al., 1993; Manzini et al., 1994). In a recently published paper (Mergny et al., 1995), it has also been shown that in the UV spectrum of i-motif-forming C-rich PO-oligos [d(CCTTTCCTTTTCCTTTCC), etc.], the absorbance increases at 265 nm and decreases at 295 nm with increasing temperature and that this behavior is indicative of thermal dissociation of the i-motif structure: Note that for some other samples such as d(TCCTCCTTTTCCTCCT), such characteristic wavelengths were slightly shifted from 275 and 305 nm to 265 and 295 nm, respectively (Mergny et al., 1995), thus implying that the appropriate observation wavelength is dependent on the sample. A similar temperature-dependent UV spectral change observed in the present investigation for PS-dC$_4$ at pH 4.5 (Figure 2a) led to the respective sharp increase and decrease in the absorbance at 275 and 305 nm, thus indicative of i-motif formation. From this plot, the T_m value was estimated to be ca. 11 °C at the strand concentration of 25 μM, which is equivalent with the value obtained by CD spectroscopy. The UV study at a strand concentration of 50 μM gave the increased T_m value of ca. 13 °C. This result indicates again that i-motif formation is concentration-dependent, and therefore, that the four-stranded structure of PS-dC$_4$ formed under the present conditions is due to intermolecular interaction.

Influence of Salt Concentration on the i-Motif Stability. CD spectroscopy performed for PS-dC$_4$ (25 μM) over 0−1 M salt concentration range at pH 4.5 and 0 °C (Figure 1d) showed a gradual decrease of the positive peaks appearing at 288 nm with an increase in the salt concentration. This trend implies that the i-motif stability of PS-dC$_4$ decreases gradually with an increase in the salt concentration and is consistent with that reported previously for C-rich PO-oligo (Mergny et al., 1995).

Difference in the i-Motif Stability between PS-dC$_4$ Diastereoisomers. PS-oligo is composed of diastereoisomers arising from the phosphorothioate P-chirality (Stec et al., 1984), and it is known that the stability of the duplex of PS-oligo with its complementary PO-oligo is dependent on the overall configuration of the PS-oligo (Kanehara et al., 1996a; Koziolkiewicz et al., 1995; LaPlanche et al., 1986; Stec et al., 1995; Stein et al., 1988). The stability of the i-motif of the diastereoisomers ($S_pS_pS_p$, $S_pR_pS_p$, and $R_pR_pR_p$) was evaluated by plotting the molar ellipticity at 288 nm, which exhibits the extent of the base stacking, against the temperature (Figure 3). The thermal dissociation CD profiles indicate that the $S_pS_pS_p$ and $R_pR_pR_p$ diastereoisomers led to the highest and lowest stability of the PS-oligo i-motif structures, respectively. It was also determined that the i-motif structure of the $S_pS_pS_p$ diastereoisomer was, however, less stable than that of PO-dC$_4$. Also, the i-motif stability of the random mixture of all eight diastereoisomers of PS-dC$_4$ was between those of $S_pS_pS_p$ and $R_pR_pR_p$. This trend is consistent with that reported previously for the stability of PS-oligo/DNA duplex (Kanehara et al., 1996a; Koziolkiewicz et al., 1995; LaPlanche et al., 1986; Stec et al., 1995; Stein et al., 1988). Consequently, P-chirality of the phosphorothioate linkage is a predominant factor for the folding of PS-dC$_n$ as well as for the duplexes between PS-oligo and DNA.

Thermal Stability of i-Motif PS-dC$_{20}$ Structure. One of the interests of this study is to see whether PS-dC$_n$ generates a stable i-motif structure under physiological conditions. For this purpose, we employed a larger sample, PS-dC$_{20}$. For a diastereomeric mixture of PS-dC$_{20}$ (6 μM), preliminary CD measurements performed at 0 and 25 °C in the absence of salt indicated great improvement of the stability of its i-motif (data not shown). This tendency is consistent with that reported previously for PO-dC$_{20}$ whose i-motif is stable even at pH 6.0 and 25 °C (Manzini et al., 1994). Then, measurements were performed at the elevated temperature of 37 °C in the presence of 0.9 wt % NaCl. The pH was varied. As represented in Figure 4a, i-motif formation was determined below pH 5.0. This result suggests that i-motif of PS-dC$_{20}$ is not sufficiently stable under normal physiological conditions, although it may be formed under rather physiologically extreme conditions such as in lysosomes, whose internal pH is estimated to be slightly acidic. At pH 4.5, the effect of the strand concentration on the stability was also studied and even a low strand concentration of 0.5 μM led to the i-motif construction (Figure 4b). In this result, the intensity of the molar ellipticity was, however, identical between the spectra above this concentration. This unex-

pected behavior can be explained to be coincidental, because CD thermal dissociation profiles obtained at strand concentrations of 2 and 7 μM were dependent on the strand concentration (Figure 4c). In this thermal dissociation plot, the different line shapes of these two T_m curves are seen. Considering the results reported previously, this may be explained reasonably by the speculation that intermolecular interaction is predominant at higher strand concentration while intramolecular folding dominates at lower concentration. If this is the case, the curve obtained at 7 μM is typical of intermolecular association and that at 0.5 μM is typical of intramolecular association. The curve produced at 2 μM may involve the contribution of these two different association modes, because this curve is analogous to that produced at 0.5 μM and shifted to higher T_m.

We also conducted gel-filtration analysis of the i-motif complex of PS-dC_{20} (Figure 5). PO-dT_{20} used as a reference produced only a single peak, which is indicative of the stretched form of this molecule. On the other hand, for PS-dC_{20}, two peaks appeared, the first peak of which was broad, suggesting i-motif formation. The second peak is possibly due to the monomeric molecules. The elution time of this peak is less than that of PO-dT_{20}. It is conceivable that PS-dC_{20} forms a more compact structure, probably through intramolecular interaction between protonated and nonprotonated cytosine moieties on the same strand, than PO-dT_{20}. Then the broad first peak is due to the folded structure. PS-dC_{20} has multiple interaction sites in one molecule, so that this molecule can form various types of folded structures with other PS-dC_{20} molecules through intermolecular interaction. Such broad distribution of i-motif PS-dC_{20} structure may account for the peak broadening. Another unusual observation was that nonannealed PS-dC_{20} gave a similar peak shape to that of the annealed sample. This may suggest that folding of PS-dC_{20} is fast compared to conventional DNA/DNA duplex formation. PO-dC_{20} also gave two peaks analogous to those of PS-dC_{20}. C-rich PO-oligos have been reported to construct a stable i-motif which could be separated by gel filtration (Leroy et al., 1993, 1994; Mergny et al., 1995). These previous data support our present understanding of the elution behavior of PS-dC_{20}. Consequently, PS-dC_{20} molecules forming four-stranded structures could be detected by gel-filtration chromatography. For further confirmation, we employed nondenaturing gel electrophoresis analysis. We observed slow migration for PS-dC_{20} in the autoradiogram compared to PO-dT_{20}, although only a weak band was obtained for PS-dC_{20}. This indicates that PS-dC_{20} was in the folded supramolecular structure. Nonannealed sample also resulted in an analogous slow band, which is consistent with the results observed in our present gel-filtration chromatography analysis.

On the basis of the above observations, we conclude that PS-dC_{20} can form a stable i-motif mixture at slightly acidic pHs even in the presence of salt and at low strand concentration, although specification of each structure is extremely difficult. In the present study, a diastereomeric mixture of PS-dC_{20} was used because isolation of PS-dC_{20} diastereoisomers is extremely hard. Enzymatic synthesis of all-R_p isomers (Hacia et al., 1994; Tang et al., 1995) and stereocontrolled chemical synthesis of PS-oligo (Stec et al., 1991 & 1995; Benimetskaya et al., 1995; Koziolkiewicz et al., 1995) have been demonstrated recently and, therefore, we are currently trying to apply such methods to the exploration of the effect of P-chirality upon the supramolecular structure of oligocytidine phosphorothioates.

In summary, as mentioned above, it is evident that PS-dC_n can form an i-motif structure similarly to C-rich PO-oligos, that its stability depends on pH, temperature, sample concentration, and concentration of salt present in the solution, and that the R_p configuration of the phosphorothioate linkage destabilizes the structure. The stability was also found to increase with an increase of the chain length: PS-dC_{20} i-motif was found to be stable even at low strand concentrations at pH 5 and 37 °C in the presence of 0.9 wt % NaCl.

REFERENCES

Agrawal, S., Goodchild, J., Civeira, M. P., Thornton, A. H., Sarin, P. S., & Zamecnik, P. C. (1988) *Proc. Natl. Acad. Sci. U.S.A. 85*, 7079−7083.

Agrawal, S., Tang, J. Y., & Brown, D. M. (1990) *J. Chromatogr. 509*, 396−399.

Ahmed, S., & Henderson, E. (1992) *Nucleic Acids Res. 20*, 507−511.

Benimetskaya, L., Tonkinson, J. L., Koziolkiewicz, M., Karwowski, B., Guga, P., Zeltser, R., Stec, W., & Stein, C. A. (1995) *Nucleic Acids Res. 23*, 4239−4245.

Burgers, P. M. J., & Eckstein, F. (1978) *Proc. Natl. Acad. Sci. U.S.A. 75*, 4798−4800.

Chen, L., Cai, L., Zhang, X., & Rich, A. (1994) *Biochemistry 33*, 13540−13546.

Edwards, E. L., Ratliff, R. L., & Gray, D. M. (1988) *Biochemistry 27*, 5166−5174.

Edwards, E. L., Patrick, M. H., Ratliff, R. L., & Gray, D. M. (1990) *Biochemistry 29*, 828−836.

Fasman, G. D. (Ed.) (1975) in *CRC Handbook of Biochemistry and Molecular Biology, 3rd edition, Nucleic Acids—Volume 1*, p 589, CRC Press, Cleveland, OH.

Gehring, K., Leroy, J. L., & Guéron, M. (1993) *Nature 363*, 561−565.

Guschlbauer, W. (1967) *Proc. Natl. Acad. Sci. U.S.A. 57*, 1441−1448.

Hacia, J. G., Wold, B. J., & Dervan, P. B. (1994) *Biochemistry 33*, 5367−5369.

Hartman, K. A., Jr., & Rich, A. (1965) *J. Am. Chem. Soc. 87*, 2033−2039.

Kanehara, H., Wada, T., Mizuguchi, M., & Makino, K. (1996a) *Nucleosides Nucleotides 15*, 1169−1178.

Kanehara, H., Mizuguchi, M., & Makino, K. (1996b) *Nucleosides Nucleotides 15*, 399−406.

Koziolkiewicz, M., Uznanski, B., Stec, W. J., & Zon, C. (1986) *Chem. Scr. 26*, 251−260.

Koziolkiewicz, M., Krakowiak, A., Kwinkowski, M., Boczkwaska, M., & Stec, W. J. (1995) *Nucleic Acids Res. 23*, 5000−5005.

LaPlanche, L. A., James, T. L., Powell, C., Wilson, W. D., Uznanski, B., Stec, W. J., Summers, M. F., & Zon, G. (1986) *Nucleic Acids Res. 17*, 1549−1561.

Leroy, J. L., Gehring, K., Kettani, A., & Guéron, M. (1993) *Biochemistry 32*, 6019−6031.

Leroy, J. L., Guéron, M., Mergny, J. L., & Hélène, C. (1994) *Nucleic Acids Res. 22*, 1600−1606.

Majumdar, C., Stein, C. A., Cohen, J. S., Broder, S., & Wilson, S. H. (1989) *Biochemistry 28*, 1340−1346.

Manzini, G., Yathindra, N., & Xodo, L. E. (1994) *Nucleic Acids Res. 22*, 4634−4640.

Matsukura, M., Shinozuka, K., Zon, G., Mitsuya, H., Reitz, M., Cohen, J. S., & Broder, S. (1987) *Proc. Natl. Acad. Sci. U.S.A. 84*, 7706−7710.

Matsukura, M., Zon, G., Shinozuka, K., Stein, C. A., Mitsuya, H., Cohen, J. S., & Broder, S. (1988) *Gene 72*, 343−347.

Mergny, J. L., Lacroix, L., Han, X., Leroy, J. L., & Hélène, C. (1995) *J. Am. Chem. Soc. 117*, 8887−8898.

Murakami, A., Tamura, Y., Wada, H., & Makino, K. (1994) *Anal. Biochem. 223*, 285−290.

Slegers, H., & Fiers, W. (1973) *Biopolymers 12*, 2007−2021.

Stec, W. J., & Wilk, A. (1994) *Angew. Chem., Int. Ed. Engl. 33*, 709−721.

Stec, W. J., Zon, G., Egan, W., & Stec, B. (1984) *J. Am. Chem. Soc. 106*, 6077−6079.

Stec, W. J., Zon, G., & Uznanski, B. (1985) *J. Chromatogr. 326*, 263−280.

Stec, W. J., Grajkowski, A., Koziolkiewicz, M., & Uznanski, B. (1991) *Nucleic Acids Res. 19*, 5883−5888.

Stec, W. J., Grajkowski, A., Kobylanska, A., Karwowski, B., Koziolkiewicz, M., Misiura, K., Okruszek, A., Wilk, A., Guga, P., & Boczkwaska, M. (1995) *J. Am. Chem. Soc. 117*, 12019−12029.

Stein, C. A., & Cheng, Y.-C. (1993) *Science 261*, 1004−1012.

Stein, C. A., Subasinghe, C., Shinozuka, K., & Cohen, J. S. (1988) *Nucleic Acids Res. 16*, 3209−3221.

Tang, J., Allysen, R., Ying, L., & Agrawal, S. (1995) *Nucleosides Nucleotides 14*, 985−990.

Wilk, A., & Stec, W. J. (1995) *Nucleic Acids Res. 23*, 530−534.

Zon, G. (1987) *J. Protein Chem. 6*, 131−145.

BI961528C